

Initiation and Abstraction Reactions in the Pyrolysis of Acetone

S. Hosein Mousavipour and Philip D. Pacey*

Department of Chemistry, Dalhousie University, Halifax, Nova Scotia, Canada B3H 4J3

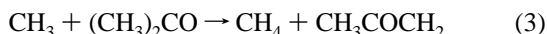
Received: July 21, 1995; In Final Form: November 17, 1995[⊗]

The rates of the reactions, $(\text{CH}_3)_2\text{CO} \rightarrow \text{CH}_3 + \text{CH}_3\text{CO}$ (1) and $\text{CH}_3 + (\text{CH}_3)_2\text{CO} \rightarrow \text{CH}_4 + \text{CH}_2\text{COCH}_3$ (3) have been studied in the flow pyrolysis of acetone at 825–940 K and 10–180 Torr. Yields of products were measured by gas chromatography. The rate constant, k_1 , for the initiation reaction, determined from the sum of the yields of the termination products, was observed to be pressure dependent at 928 K. The Arrhenius expression for this reaction at the high-pressure limit (obtained from a nonlinear least-squares fit to the experimental data using the Troe factorization procedure) was found to be $k_{1\infty} (\text{s}^{-1}) = 10^{17.9 \pm 0.8} \exp(-353 \pm 14 \text{ kJ mol}^{-1}/RT)$. The Troe method has also been used to find the high-pressure limits of the cross-combination ratio for CH_3 and CH_3COCH_2 radicals (1.9 ± 0.1) and of the quotient k_5/k_3^2 , where reaction 5 is $2\text{CH}_3 \rightarrow \text{C}_2\text{H}_6$. Calculated rate constants for reaction 3, when combined with values reported from photolysis experiments at lower temperatures, were found to exhibit a curved Arrhenius plot. A transition state theory model was fitted to the data for k_3 to determine the average transitional vibrational term value in the transition state ($279 \pm 8 \text{ cm}^{-1}$), the effective activation barrier height ($46 \pm 1 \text{ kJ mol}^{-1}$), and the full width of the barrier at half its height ($52 \pm 3 \text{ pm}$).

Introduction

“The photolysis of acetone is undoubtedly the most studied reaction in gas kinetics,” according to a review.¹ The objective of at least 36 of these studies has been to measure the rate constant for the reaction of methyl radicals with acetone or other organic molecules. However, such studies have been limited to the temperature range 300–750 K. It is the purpose of the present work to build on this firm foundation, extending the temperature range up to 940 K, generating methyl radicals not by photolysis, but by the pyrolysis of acetone.

Rice and Herzfeld² proposed that the pyrolysis of acetone proceeds by a free radical mechanism



It has been confirmed that CH_4 and CH_2CO are the major products of the reaction,³ but there do not appear to have been any experimental studies of all the minor products.

Applying the steady state approximation to the radicals in this mechanism, the rate of the initiation reaction, step 1, would be equal to the sum of the rates of the termination reactions, steps 5–7. This assumption would allow the calculation of the rate constant, k_1 , for reaction 1 as

$$k_1 = (R_e^{ss} + R_b^{ss} + R_h^{ss})/[(\text{CH}_3)_2\text{CO}] \quad (8)$$

Here R_e^{ss} , R_b^{ss} , and R_h^{ss} are the steady state rates of formation of the termination products ethane, butanone, and 2,5-hexanedione, respectively.

Again applying the steady state approximation, k_5/k_3^2 may be calculated as

$$k_5/k_3^2 = R_e^{ss}[(\text{CH}_3)_2\text{CO}]^2/(R_m^{ss})^2 \quad (9)$$

where R_m^{ss} is the steady state rate of formation of methane. This equation has been the basis of the determination of k_3 in most photolysis experiments.¹ Reaction 5 has been studied many times, and the pressure and temperature dependence of its rate constant are reasonably well-known.⁴ In this work we will attempt to apply eqs 8 and 9 to the pyrolysis of acetone for the first time.

The present experiments employed a flow reactor system. Acetone entered the reactor cold, and the steady rates of product formation would only have been achieved after a delay, τ_h , in transferring heat to the flowing gas and after a delay, τ_c , as reaction 1 increased the concentrations of radicals toward their steady state values. During the delay caused by incomplete radial heat transfer, the observed chordal or average rate of methane formation, R_m^{app} ($=[\text{CH}_4]/t$), would have been given by the following expression⁵

$$R_m^{\text{app}}/R_m^{ss} = 1 - (\tau_h/t) \quad (10)$$

During the establishment of the steady state for radicals, the observed rate of formation of methane would have been given by⁶

$$R_m^{\text{app}}/R_m^{ss} = (\tau_c/t \ln 2) \ln \cosh(t \ln 2/\tau_c) \quad (11)$$

Any pressure dependence of the rate constants k_1 and k_5 can be analyzed using the factorization method of Troe:⁷

$$k_1/k_{1\infty} = F_{\text{LH}} F_{\text{C}}^{\text{SC}} F_{\text{C}}^{\text{WC}} \quad (12)$$

$$F_{\text{LH}} = (k_{1,0}[\text{M}]/k_{1\infty})/(1 + k_{1,0}[\text{M}]/k_{1\infty}) \quad (13)$$

Here $k_{1\infty}$ and $k_{1,0}$ are the limiting, high-pressure, first-order and

[⊗] Abstract published in *Advance ACS Abstracts*, February 1, 1996.

limiting, low-pressure, second-order rate constants, respectively, for reaction 1. Parallel expressions are available for reaction 5, but the rate constants are second and third order, respectively. F_c^{SC} corrects for strong collision effects. The weak collision factor, F_c^{WC} , is a function of the collision efficiency, β_c , and was calculated using eqs 79–81 in ref 7. The effective number of vibrational modes, S_k , was calculated from experimental vibrational frequencies, as listed in the Appendix in the supporting information.

The steady rate of formation of the cross-combination product, butanone, should be approximately twice the square root of the product of the other termination rates, provided all reactions are at their high-pressure limits.⁸ At lower pressures, this relationship could be generalized as follows:

$$R_b^{ss} = m(R_e^{ss} R_h^{ss})^{1/2} \quad (14)$$

We will make use of this relationship to estimate rates of termination reactions in conditions where direct measurements were not possible.

Experimental Section

Acetone (Burdick & Jackson, 99.9%) was degassed by condensing with liquid nitrogen, evaporated, and was again degassed in liquid nitrogen. Methane and ethane of 99% purity (Matheson CP Grade) were used to prepare a mixture to calibrate the gas chromatograph. Butanone (Fisher) and 2,5-hexanedione (Eastman Kodak Co.) with less than 1% acetone as impurity were used individually for the same purpose.

The flow system was similar to that used previously in this laboratory.^{5,6} The pressures in the storage bulbs and reactor were monitored by two pressure transducers (Bell & Howell, Type 4-366-0006-03Mo, 0–50 and 0–15 psi). The flow rate into the reactor was controlled by a needle valve (Edwards, Model LBIB). Three 1-m cylindrical quartz reactors were used: two with internal radii of 4.0 and 3.0 mm and inside thermocouple wells of 2.1 mm external radius and the third with a 1.4 mm internal radius and an outside thermocouple compartment. The surface-to-volume ratios (s/v) for these reactors were calculated to be 10.3, 20.4, and 14.0 cm^{-1} , respectively. During an experiment, a 43 cm long section was heated by a resistive furnace. The reactor temperature was controlled by a platinum/platinum–13% rhodium thermocouple. An automatic controller, which consisted of a pressure transducer (MKS-122AA-01000AB), a programmable temperature controller (Omega CN 2000), and an outlet selenoid valve (MKS-0248A-50000SY), was used to control the pressure in the reactor.

A six-way linear gas sampling valve (Varian 57-000034-00) was used to take samples in a 10 cm^3 sample loop, and a gas chromatograph (Tracor 550) was used to analyze the samples. Methane, ethane, and ethylene were separated on a 1-m silica gel column (mesh 100/120) at room temperature, CO and hydrogen on a 1.2 m alumina column (type F1) at 0 °C, butanone on a 1.2 m Porapak column (type Q) at 160 °C, and 2,5-hexanedione on a 1.0 m 10% carbowax-20M on chromosorb column at 110 °C. Nitrogen was used as carrier gas. A flame ionization detector was used to detect the hydrocarbon and ketone products, and a zirconia sensor⁹ was used to detect CO and hydrogen. Typically three samples were analyzed at each flow condition; reproducibility was between 0.5% and 3%, except for the smallest peaks. Ketene peaks at 2150 cm^{-1} were detected with a (Nicolet 510P FT-IR) spectrometer with a resolution of 4 cm^{-1} . All analytical techniques were not applied to all samples.

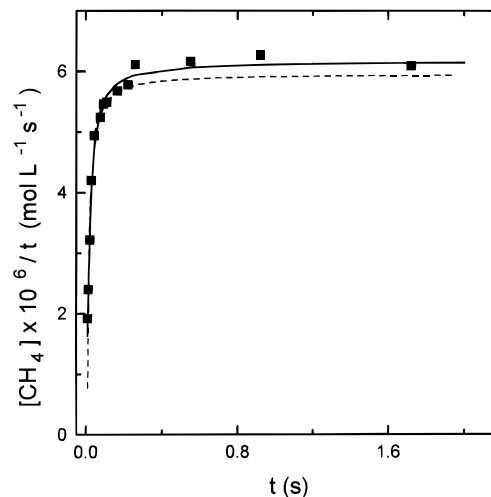


Figure 1. Chordal rate of formation of CH_4 at 20 Torr and 876 K in a reactor with a surface-to-volume ratio of 14.0 cm^{-1} : ■, experimental data; lines, nonlinear least-squares fits of eqs 10 (dashed) and eq 11 (solid) to the data.

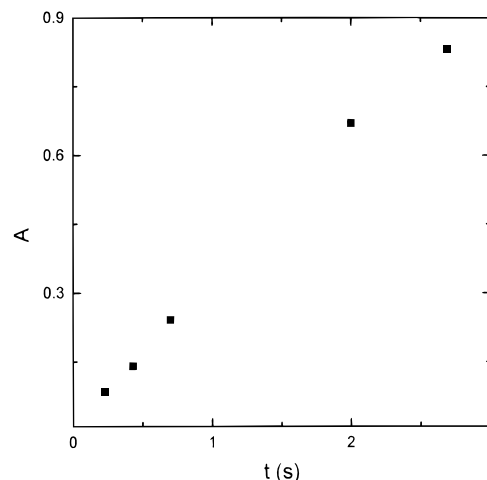


Figure 2. Ketene absorbance at 2150 cm^{-1} as a function of residence time at 876 K and 125 Torr with an s/v of 14.0 cm^{-1} .

Results

The reaction was studied in the temperature range 825–940 K, the pressure range 10–180 Torr, and the residence time range 0.01–3 s. The main products observed were methane and ketene, and the minor products were hydrogen, carbon monoxide, ethylene, ethane, propylene, propane, butanone, and 2,5-hexanedione. Conversions were less than 1%.

Figure 1 shows the chordal rate of formation of methane at 876 K and 20 Torr. There was an initial rise in the rate, followed by a plateau at times longer than 0.3 s. Both eqs 10 and 11 were fitted to the data from this experiment and similar experiments by nonlinear least squares;¹⁰ the difference between the steady state rates obtained from one set of data with the two equations was always less than 5%. At conditions where no induction period was observed, the average rate of formation in the plateau region was taken as the steady state rate of formation.

Figure 2 shows the absorbance by ketene at 2150 cm^{-1} as a function of residence time at 876 K and 125 Torr. Similar experiments were performed at temperatures from 834 to 929 K and pressures between 85 and 176 Torr. The ketene infrared absorbance was always proportional to the methane gas chromatographic peak size, independent of reaction pressure and temperature. Assuming the steady rates of formation of methane

TABLE 1: Steady State Rates and Rate Constants from Experiments at Several Pressures and Temperatures in Three Reactors

P , Torr	$R_m \times 10^5$, $\text{mol L}^{-1} \text{s}^{-1}$	$R_e \times 10^7$, $\text{mol L}^{-1} \text{s}^{-1}$	$R_b \times 10^7$, $\text{mol L}^{-1} \text{s}^{-1}$	$R_h \times 10^7$, $\text{mol L}^{-1} \text{s}^{-1}$	$k_5/k_3^2 \times 10^4$, mol s L^{-1}	$k_1 \times 10^4$, s^{-1}
928 K, $s/v = 20.4 \text{ cm}^{-1}$						
10.3	1.37	7.0	3.2	0.21	1.18 ± 0.08	58 ± 2
20.9	3.67	15.8	7.2	0.49	1.53 ± 0.08	65 ± 1
41.4	11.0	39.	16.3	1.23	1.65 ± 0.07	79 ± 2
82.2	25.7	73.	39.4	4.1	2.2 ± 0.2	82 ± 2
126.0	46.	107.	81.	12.0	2.4 ± 0.2	92 ± 2
182.0	76.	161.	109.	17.0	2.8 ± 0.2	91 ± 1
876 K, $s/v = 10.3 \text{ cm}^{-1}$						
10.3	0.22	0.40	0.41		3.0 ± 0.3	4.6 ± 0.2
20.6	0.62	1.08	0.78		4.0 ± 0.2	5.2 ± 0.1
30.6	0.99	1.62	1.13		5.2 ± 0.3	
41.3	1.40	1.81	1.54		5.3 ± 0.2	4.7 ± 0.1
876 K, $s/v = 20.4 \text{ cm}^{-1}$						
20.5	0.61	1.05			4.0 ± 0.4	
30.8	0.95	1.33			4.7 ± 0.3	
41.0	1.49	1.89	1.60		4.8 ± 0.1	4.9 ± 0.1
82.0	3.27	2.92	3.7		6.1 ± 0.2	5.1 ± 0.1
876 \pm 2 K, $s/v = 14.0 \text{ cm}^{-1}$						
10.3				0.059		
20.6	0.62	1.13		0.090	4.2 ± 0.8	
41.3	1.43	1.79		0.223	5.0 ± 0.2	
81.4	3.70	3.3		1.03	5.4 ± 0.2	
124.0	5.9	3.9	5.5	1.81	5.7 ± 0.2	4.9 ± 0.1
176.0	9.5	5.9	8.8	2.92	6.8 ± 0.3	5.5 ± 0.1
834 \pm 2 K, $s/v = 10.3 \text{ cm}^{-1}$						
10.3	0.039	0.039	0.087		10 ± 2	0.81 ± 0.04
21.0	0.098	0.072	0.190		13 ± 1	0.84 ± 0.03
41.5	0.24	0.122	0.323		14 ± 2	0.74 ± 0.02
80.6	0.44	0.163			20 ± 2	
126.9	0.88	0.238			18 ± 2	
183.6	1.46	0.361			21 ± 2	

^a R_m , R_e , R_b , and R_h are the rates of formation of methane, ethane, butanone, and 2,5-hexanedione, respectively. s/v is the reactor surface-to-volume ratio.

TABLE 2: Results of Experiments Carried out at 15.5 Torr at Several Temperatures with s/v Equal to 10.3 cm^{-1}

T , K	$R_m \times 10^6$, $\text{mol L}^{-1} \text{s}^{-1}$	$R_e \times 10^8$, $\text{mol L}^{-1} \text{s}^{-1}$	$R_b \times 10^8$, $\text{mol L}^{-1} \text{s}^{-1}$	$R_h \times 10^8$, $\text{mol L}^{-1} \text{s}^{-1}$	k_5/k_3^2 , mol s L^{-1}	k_1 , s^{-1}
940	45.4	230	108	9.4	7.8×10^{-5}	1.31×10^{-2}
897	9.23	28.5	18.7		2.57×10^{-4}	1.77×10^{-3}
854	1.63	1.97	3.35		6.3×10^{-4}	2.12×10^{-4}
825	0.44	0.32	1.06		1.49×10^{-3}	

and ketene were equal, as predicted by the mechanism (reactions 3 and 4) provided chains are long, the molar absorption coefficient of ketene was calculated to be $535 \pm 36 \text{ L mol}^{-1} \text{ cm}^{-1}$. Here the quoted uncertainty is the standard deviation of 29 individual ketene/methane measurements.

Hydrogen, ethylene, propane, and propylene were secondary products, with yields proportional to the square of the residence time. Hydrogen was detected in clean reactors only at pressures higher than 80 Torr, but was also detected at lower pressures when the reactor surface was partially covered by carbon.

Experiments were carried out at 876 K in each of the three reactors to test for any surface reaction. Carbon deposition on the reactor wall increased the yield of ethylene but, as Table 1 shows, with clean quartz reactors at identical pressures; there was no trend evident in the steady state rates of formation of methane, ethane, and butanone on changing s/v . The last digit quoted in each rate is the first digit of the standard deviation.

Table 2 shows the results of experiments at different temperatures at a constant pressure of 15.5 Torr.

Equation 9 was used to calculate the values of k_5/k_3^2 for several conditions. Figure 3 shows the pressure and temperature dependences of this quotient. The value of k_5 is known to be affected by changing the pressure.⁴ Values of the Troe input

parameters, S_k , B_T , and F_C^{SC} , for reaction 5 are given in the Appendix. The Troe expression (12) for the pressure dependence was fitted to the data by nonlinear least squares,¹⁰ to estimate the high- and low-pressure limits for k_5/k_3^2 . The high-pressure limits for this quotient at 928, 876, and 834 K, assuming unit collision efficiency, are presented in Table 3. Changing the fixed value of β_C from unity to 0.1 changed these values by only 15%. The uncertainties in these numbers in Table 3 are standard deviations determined by the least-squares program.¹⁰ The low-pressure limits for k_5/k_3^2 were calculated to be 8 ± 2 , 25 ± 3 , and $66 \pm 17 \text{ s}$ at 928, 876, and 834 K, respectively. The ratios of $(k_5/k_3^2)_\infty$ to k_5/k_3^2 at 15.5 Torr were calculated to be 2.75, 2.66, and 2.62 at 928, 876, and 834 K, respectively. Values of $(k_5/k_3^2)_\infty$ at 940, 897, 854, and 825 K were calculated by multiplying the values of k_5/k_3^2 at 15.5 Torr in Table 2 by the ratios at the nearest temperature in the preceding sentence.

It was not possible to separately determine k_3 and k_5 from the present experiments, so a value of $k_{5\infty}$ was taken from the literature,¹¹ ($k_{5\infty} (\text{L mol}^{-1} \text{ s}^{-1}) = 9.05 \times 10^{13} (T/\text{K})^{-1.18} \exp(-2.74 (\text{kJ mol}^{-1})/RT)$). The values of k_3 in Table 3 were calculated by substituting these values of $k_{5\infty}$ into the values of $(k_5/k_3^2)_\infty$ in the preceding column. The results are shown as the filled squares in Figure 4.

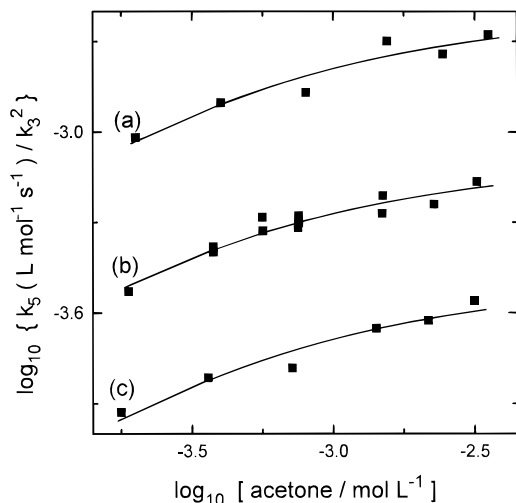


Figure 3. Dependence of the ratio, k_5/k_3^2 , on temperature and acetone concentration: ■, experimental data; a, 834 K; b, 876 K; c, 928 K; —, nonlinear least-squares fits of eq 12 with unit collision efficiency.

TABLE 3: Limiting Rate Constants at Several Temperatures

<i>T</i> , K	$k_{1\infty}$, s ⁻¹	$(k_5/k_3^2)_\infty \times 10^4$, mol s L ⁻¹	$k_3 \times 10^{-6}$, L mol ⁻¹ s ⁻¹
940	$(2.4 \pm 0.2) \times 10^{-2}$	2.2 ± 0.2	9.5 ± 0.5
928	$(1.2 \pm 0.1) \times 10^{-2}$	3.7 ± 0.3	7.4 ± 0.3
897	$(2.7 \pm 0.2) \times 10^{-3}$	7.4 ± 0.6	5.3 ± 0.2
876	$(5.8 \pm 0.3) \times 10^{-4}$	9.3 ± 0.5	4.8 ± 0.1
854	$(2.5 \pm 0.1) \times 10^{-4}$	17 ± 1	3.6 ± 0.1
834	$(8.8 \pm 0.6) \times 10^{-5}$	29 ± 3	2.8 ± 0.2
825		39 ± 4	2.4 ± 0.2

The butanone and 2,5-hexanedione peaks were not measured at some experimental conditions, represented by blanks in Tables 1 and 2. Where peaks were reliably measured for all three termination products (if necessary, including data from two reactors), eq 14 was applied to calculate values of the cross-combination ratio, m . This ratio was found to be weakly dependent on pressure, as predicted in the Introduction because of the known pressure dependence of k_5 . Accordingly, m^{-2} , which is proportional to k_5 , was plotted in graphs like Figure 3. The pressure dependence was found to be similar to, but slightly weaker than, that for k_5/k_3^2 . The results were treated by the Troe factorization method as described for k_5/k_3^2 . The limiting high-pressure values of m were found to be 1.9 ± 0.1 at both 928 and 876 K.

For conditions where one termination product was not measured, a value of m determined at the nearest possible temperature and pressure was inserted in eq 14, which was then solved for the missing rate. This was not done at 825 K, where it appeared that the missing rate could have been the major radical recombination. The rate constant for reaction 1 was calculated using the sum of the rates of formation of termination products as in eq 8. Values of this rate constant listed in Table 1 and shown in Figure 5 have a clear dependence on pressure at 928 K and a slight dependence at 876 K. Troe input parameters for this reaction are also given in the supporting information. The Troe expression, eq 12, was fitted to the experimental data by nonlinear least squares¹⁰ to estimate the low- and high-pressure limits, $k_{1,0}$ and $k_{1\infty}$. The results showed that $k_{1\infty}$ was not sensitive to F_C^{WC} and that changing β_c , the collision efficiency, from unity to 0.1 again changed $k_{1\infty}$ by only 15%. The value of $k_{1,0}$ at 928 K was found to be $(1.0 \pm 0.2) \times 10^3$ L mol⁻¹ s⁻¹, but the value at 876 K could not be reliably determined. The high-pressure limits for k_1 are given in Table 3. To calculate $k_{1\infty}$ at the temperatures in Table 2, where

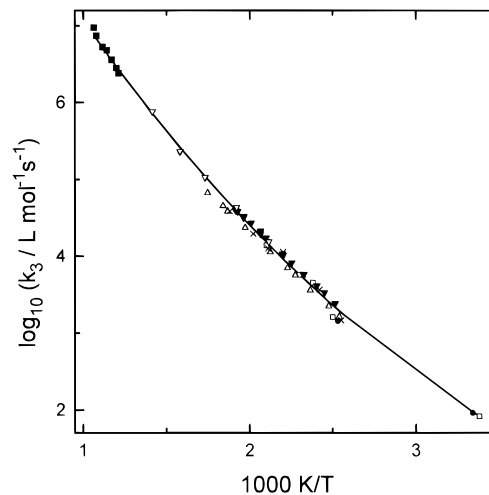


Figure 4. Overall temperature dependence of k_3 : ■, this work; ▼, ref 25a; ×, ref 25b; △, ref 25c; ●, ref 25d; □, ref 25e; ▽, ref 14; —, nonlinear least-squares fit of eq 16 to the experimental data.

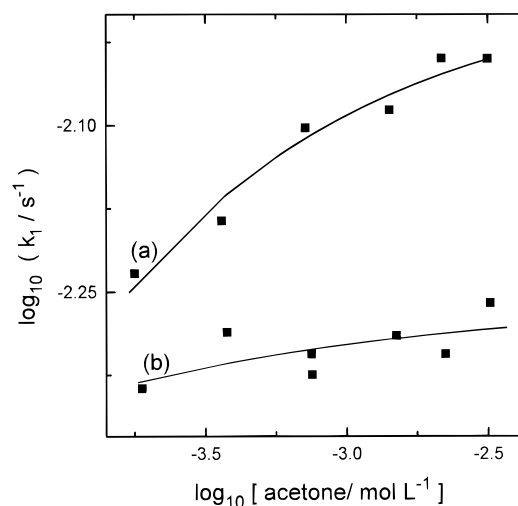


Figure 5. Dependence of k_1 on acetone concentration: a, 928 K; b, 876 K (raised 1 log unit); ■, experimental data; —, nonlinear least-squares fit of eq 12 to the data with $\beta_c = 1.0$.

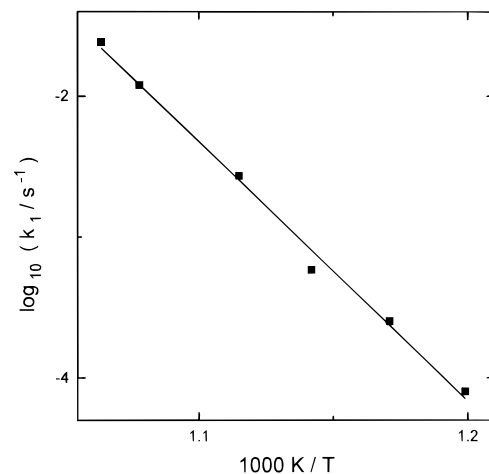


Figure 6. Dependence of the high-pressure limit of k_1 on temperature: ■, experiment; —, linear least-squares fit.

measurements were made at only a single pressure, values of $k_1/k_{1\infty}$ at 15.5 Torr were taken from the curves at the nearest temperature or temperatures in Figure 5.

An Arrhenius plot for $k_{1\infty}$ is shown in Figure 6. The Arrhenius expression for this rate constant from the present work

was found by least squares to be

$$k_{1\infty} (\text{s}^{-1}) = 10^{17.9 \pm 0.8} \exp(-353 \pm 4 \text{ kJ mol}^{-1}/RT)$$

Discussion

Fits of both eqs 10 and 11 to the data obtained during the induction periods gave consistent values of the plateau rates within 5%. At most experimental temperatures and pressures, we were able to make measurements in the steady state regime.

It is necessary to consider whether reactions in addition to (1) to (7) could have contributed to the observed products. A possible competitor to the initiation reaction 1 is the rupture of a carbon-hydrogen bond in acetone. However, the dissociation enthalpy for this bond is 411 kJ mol^{-1} ,¹² 72 kJ mol^{-1} greater than that calculated for reaction 1. Such a difference would lead to a ratio of 4 orders of magnitude in the exponential factors at the present experimental temperatures.

It is also necessary to consider possible competing termination processes. It has been suggested¹³ that there is a disproportionation reaction ($\text{CH}_3 + \text{CH}_3\text{COCH}_2 \rightarrow \text{CH}_4 + \text{CH}_2\text{COCH}_2$) with a rate about one-quarter the rate of reaction 6. However, one suggested product was a diradical, which seems improbable. Another suggestion,¹⁴ ($\text{CH}_3 + \text{CH}_3\text{COCH}_2 \rightarrow \text{C}_2\text{H}_4 + \text{CH}_4 + \text{CO}$), can be ruled out because C_2H_4 was not a primary product in the present study. The CH_3CO radical could participate in termination. Using a value of k_2 from the literature,¹⁵ we estimate that the concentration of this radical is always at least 4 orders of magnitude less than that of CH_3 under the present experimental conditions. Addition of CH_3 to acetone would produce the $(\text{CH}_3)_2\text{CO}$ radical. Using reported rate constants for the forward and reverse processes,^{16,17} we predict that the concentration of this radical would be several orders of magnitude lower still.

Variation, like that observed in Figure 3, of the quotient, k_5/k_3^2 , with changing acetone concentration has previously been observed in photolysis experiments. Brinton¹⁴ performed the most detailed study and criticized previous investigations, particularly those at temperatures above 600 K. In order to explain values of m as low as 0.3 and variations of k_5/k_3^2 by a factor of 7 with only a 4-fold pressure change (but a 25-fold photolysis intensity change), the following additional reaction was postulated:



We need to carefully consider the pressure dependence of m and k_5/k_3^2 to determine whether reaction (15) could have an effect under the present conditions.

The values of $P_{1/2}$, the pressure at which k_5 has fallen to half its high-pressure limiting value, were found from the variation of k_5/k_3^2 in Figure 3 to be 39, 42, and 49 Torr at 834, 876, and 928 K, respectively, and, from m^{-2} , to be 12 and 10 Torr at 876 and 928 K, respectively. These may be compared with a value of 17 Torr found for reaction 5 at 822 K,¹⁸ and values between 10 and 60 Torr in the present temperature range from a survey of the literature for the reverse reaction.¹⁹

We have fitted a model in which C_2H_6 is formed by both reactions 5 and 15 to the pressure dependence of the present measurements of $R_e^{\text{ss}}[(\text{CH}_3)_2\text{CO}]^2/(R_m^{\text{ss}})^2$ (the right-hand side of eq 9), as listed in the second last column in Table 1. The pressure dependence of reaction 5 was assumed to follow refs 18 and 19. The fitted rates of reaction 15 were small enough to affect the quoted values of k_3 by 10% or less.

Addition of toluene, a radical scavenger, to the pyrolysis of acetone²⁰ suppressed the formation of ketene to only 10–15%

of the yield of CO from reaction 2, and the latter reaction was found to have a rate only 10% or less of the rates of formation of methane and ketene in the present work. Thus, a direct, unimolecular production of ketene and methane from acetone (without the participation of radicals) could only account for 1% of the methane observed in this work.

The value of 1.9 ± 0.1 found in this work for the cross-combination quotient of CH_3 and CH_3COCH_2 radicals is similar to the values of 2.4, 2.0, 1.8 ± 0.1 , 1.9 ± 0.2 , and 2.4 ± 0.2 found in photolysis experiments¹⁴ at temperatures of 473, 523, 578, 638, and 708 K, respectively. It is also similar to values of 1.86–2.08 determined for various alkyl radicals at room temperature.⁸ According to simple collision theory, this quotient would be equal to the product of a factor of 2 from symmetry, a factor of 1.11 from the quotient of relative velocities, and an undetermined factor close to unity from the quotient of collision diameters. It is not possible to determine these three rate constants separately from the present results.

Our Arrhenius parameters for $k_{1\infty}$, $\log A = 17.9 \pm 0.8$, and $E_A = 353 \pm 14 \text{ kJ mol}^{-1}$, are similar to the values reported by Ernst and Spindler²¹ from shock tube experiments, $\log A = 16.4$ and $E_A = 342 \pm 12 \text{ kJ mol}^{-1}$. These authors also noted that the rate constant was pressure dependent. The preexponential factors, $\log A = 14.4$ and 14.1 , reported²⁰ from toluene carrier experiments, are lower than expected for a unimolecular decomposition reaction.

If we assume that the temperature dependence of the reverse of reaction 1 is between $+RT/2$ and $-RT/2$, its activation energy would be $0 \pm 4 \text{ kJ mol}^{-1}$. Combining this with the present activation energy for reaction 1, we obtain $353 \pm 15 \text{ kJ mol}^{-1}$ as the internal energy change for reaction 1 and $360 \pm 15 \text{ kJ mol}^{-1}$ as the enthalpy change. Taking heat capacities from the literature, the latter value may be adjusted to $358 \pm 15 \text{ kJ mol}^{-1}$ at 298 K. Combining this with the heats of formation of acetone²² and CH_3 ,²³ we obtain $-6 \pm 15 \text{ kJ mol}^{-1}$ as the heat of formation of CH_3CO . This may be compared with the recent determination of $-10.0 \pm 1.2 \text{ kJ mol}^{-1}$.²⁴

The experimental data for k_3 from Table 3 were combined in Figure 4 with data at lower temperatures from the literature, consistently taking $k_{5\infty}$ from ref 11. There is good agreement among the results of photolysis experiments in the temperature range 400–550 K,¹ so only three such studies^{25a–c} have been selected. Between 550 and 750 K, only the data from the most detailed study¹⁴ have been included.

The Arrhenius plot for reaction 3 in Figure 4 is curved. Similar curvature has been observed previously in a number of reactions involving hydrogen transfer.^{4,26} For several reactions it has been possible to fit a transition state theory model to the experimental data.²⁶

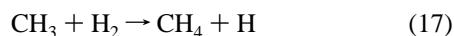
$$k = \kappa(T/T^*, V_b)(k_B T/h)\delta Q_{\text{TS}}(I, \omega_b, T)/Q_A Q_B \exp(-V_b/RT) \quad (16)$$

where $\kappa(T/T^*, V_b)$ is the tunneling factor, δ is the reaction path degeneracy, k_B is Boltzmann's constant, T is the absolute temperature, h is Planck's constant, Q_{TS} , Q_A , and Q_B are partition functions for the transition state (TS) and reactants (A and B), and V_b is the effective barrier height including zero-point energy. The characteristic tunneling temperature, T^* , is the temperature at which the average reacting pair has energy approximately equal to half the barrier height. $Q_{\text{TS}}(I, \omega_b, T)$ depends on the product of moments of inertia, I , of the transition state and on the average term value, ω_b , for six transition state vibrational degrees of freedom which are significantly different from the corresponding motions in the reactants. The moments of inertia

in the transition state were calculated from the results of a semiempirical bond energy–bond order (BEBO) calculation.²⁷

General features of the transition state theory method have been described elsewhere. Details specific to reaction 3 are given in the Appendix in the supporting information.^{26–33} The three parameters V_b , T^* , and ω_b , in eq 16 were fitted to the experimental data by nonlinear least squares.¹⁰ The parameters were found to be equal to 46.0 ± 1.0 kJ mol⁻¹, 375 ± 17 K, and 279 ± 8 cm⁻¹, respectively.

These results could be compared with those for reaction 17:²⁶



Parameters for this reaction, updated by including recent experimental results,³⁴ are 58.5 ± 1.2 kJ mol⁻¹, 395 ± 36 K, and 806 ± 33 cm⁻¹, respectively. Reaction 3 is exoergic by 27 kJ mol⁻¹ and would be expected to have a lower activation barrier than reaction 17, which is almost thermoneutral.²⁶ Half the difference in exoergicity is reflected in the barrier height in the forward direction and half, in the reverse barrier height.

The values of T^* , defined in terms of the second derivative of potential energy with respect to the reaction coordinate at the barrier top, are similar to each other. The full widths, $\Delta s_{1/2}$, of the Eckart barriers at half their heights²⁶ were calculated from V_b and T^* to be 52 ± 3 pm for reaction 3 and 58 ± 5 pm for reaction 17.

The average vibrational term value in the transition state for reaction 3 could have been predicted to be lower than that for reaction 17 because of the heavier CH₃COCH₂ replacing a hydrogen atom and because of the contribution of a hindered internal rotation in the TS for reaction 3. However, the more than 2-fold drop is surprising. In fact, the present value of ω_b is the lowest we have found for any reaction.²⁶

The barrier height is within 10% of the value of 51 kJ mol⁻¹ estimated by the BEBO method in the supporting information. It is only about two-thirds of the experimental activation energy of 72 kJ mol⁻¹ found in the present work between 825 and 940 K. This difference may be explained in terms of the low-frequency vibrations in the activated complex. We consider that three translational degrees of freedom of the reactants, plus two rotations and two vibrations (a C–H stretch and a hindered methyl internal rotation) transform in the complex to the reaction coordinate and six low-frequency vibrations (the symmetric stretch, a similar hindered internal rotation, two CHC bends, and two CH₃ rocks). (The rotation of the reactant CH₃ about its 3-fold axis is considered to remain effectively free in the complex.) The above seven degrees of freedom will each contribute thermal energy close to RT in the activated complex. Their net contribution to the activation energy would be $3.5RT$, or 25 kJ mol⁻¹, just enough to account for the difference between the observed activation energy and the barrier height fitted to the data.

On the other hand, in photolysis experiments at 400–500 K, the observed activation energy was 40 ± 1 kJ mol⁻¹, which is less than the present barrier height. At such temperatures tunneling allows significant amounts of reaction by species with less energy than the barrier height.

The curvature of the Arrhenius plot can thus be understood in terms of the contribution of tunneling at low temperatures and of the low-frequency vibrations at higher temperatures. It is anticipated that similar statements will apply to reactions of methyl radicals with other organic molecules.

In summary, the pyrolysis of acetone is seen to behave as predicted by the Rice–Herzfeld mechanism; the major products are methane and ketene and the minor primary products are

ethane, CO, butanone, and 2,5-hexanedione. The relative rates of formation of the termination products are in good agreement with the simple predictions of collision theory, provided a small adjustment is made for the pressure dependence of at least one of these rate constants. The initiation rate constant, determined from the sum of the termination rates, depends weakly on pressure and has an activation energy in reasonable agreement with recent thermochemistry. The abstraction of hydrogen from acetone by methyl radicals has a strongly curved Arrhenius plot, which has been interpreted to provide new insights into the role of tunneling and of six low-frequency vibrations in the transition state.

Acknowledgment. The authors thank the Natural Sciences and Engineering Research Council of Canada for financial support, the Ministry of Culture and Higher Education of Iran for a scholarship to S.H.M., N. Burford for the use of the infrared spectrometer, and V. Knyazev for sending results prior to publication.

Supporting Information Available: A description of the Troe model and input parameters for reactions 1 and 5 and a description of the transition state theory treatment of reaction 3 with a table of input parameters (5 pages). Ordering information is given on any current masthead page.

References and Notes

- (1) Kerr, J. A.; Parsonage, M. J. *Evaluated Kinetic Data on Gas Phase Hydrogen Transfer Reactions of Methyl Radicals*; Butterworths: London, 1976; p 171.
- (2) Rice, F. O.; Herzfeld, K. F. *J. Am. Chem. Soc.* **1934**, *56*, 284.
- (3) Rice, F. O.; Vollrath, R. E. *Proc. Natl. Acad. Sci.*, **1929**, *15*, 702.
- (4) Rice, F. O.; Varnerin, R. E. *J. Am. Chem. Soc.* **1955**, *77*, 221. McNesby, J. R.; Davis, T. W.; Gordon, A. S. *J. Am. Chem. Soc.* **1954**, *76*, 823, 956.
- (5) Baulch, D. L.; Cobos, C. J.; Cox, R. A.; Esser, C.; Frank, P.; Just, Th.; Kerr, J. A.; Pilling, M. J.; Troe, J.; Walker, R. W.; Warnatz, J. *J. Phys. Chem. Ref. Data* **1992**, *21*, 655.
- (6) Furue, H.; Pacey, P. D. *J. Phys. Chem.* **1980**, *84*, 3139.
- (7) Pacey, P. D.; Wimalasena, J. H. *J. Phys. Chem.* **1984**, *88*, 5657.
- (8) Troe, J. *J. Phys. Chem.* **1979**, *83*, 114.
- (9) Terry, J. O.; Futrell, J. H. *Can. J. Chem.* **1967**, *45*, 2327; **1968**, *46*, 664.
- (10) Pacey, P. D.; Furue, H. PCT International Patent Application, 1994, Publication number WO94/29709.
- (11) Ralston, M. In *BMDP Statistical Software*; Dixon, W. J., Ed.; University of California Press: Berkeley, 1983; p 305.
- (12) Wagner, A. F.; Wardlaw, D. M. *J. Phys. Chem.* **1988**, *92*, 2462.
- (13) Slagle, I. R.; Gutman, D.; Davies, J. W.; Pilling, M. J. *J. Phys. Chem.* **1988**, *92*, 2455.
- (14) Kerr, J. A. *Handbook of Chemistry and Physics*, 75th ed.; Lide, D. R., Ed.; CRC Press: Boca Raton, FL, 1995; 9-64.
- (15) Darwent, B. deB.; Allard, M. J.; Hartman, M. F.; Lange, L. J. *J. Phys. Chem.* **1960**, *60*, 1847.
- (16) Brinton, R. K. *J. Am. Chem. Soc.* **1961**, *83*, 1541.
- (17) Benscira, A.; Knyazev, V. D.; Slagle, I. R.; Gutman, D.; Tsang, W. *Ber. Bunsen-Ges. Phys. Chem.* **1992**, *96*, 1338.
- (18) Knoll, H.; Richter, G.; Schliebs, R. *Int. J. Chem. Kinet.* **1980**, *12*, 623.
- (19) Heicklen, J. *Adv. Photochem.* **1988**, *14*, 177.
- (20) Pacey, P. D.; Wimalasena, J. H. *J. Phys. Chem.* **1980**, *84*, 2221.
- (21) Cao, J.-R.; Back, M. H. *J. Phys. Chem.* **1984**, *88*, 3074.
- (22) Szwarc, M.; Taylor, J. W. *J. Chem. Phys.* **1955**, *23*, 2310. Clark, D.; Pritchard, H. O. *J. Chem. Soc.* **1956**, 2136.
- (23) Ernst, J.; Spindler, K. *Ber. Bunsen-Ges. Phys. Chem.* **1975**, *79*, 1163. Ernst, J.; Spindler, K. *Ibid.* **1976**, *80*, 645.
- (24) Gurvich, L. V.; Iorish, V. S.; Yangman, V. S.; Dorofeeva, O. V. *Handbook of Chemistry and Physics*, 75th ed.; Lide, D. R., Ed.; 1995; pp 5–55.
- (25) Chase, M.; Davies, C.; Downey, J.; Frurip, D.; McDonald, A.; Syverud, A. *JANAF Thermochemical Tables*; *J. Phys. Chem. Ref. Data, Suppl. 1* **1985**, 14.
- (26) Niiranen, J. T.; Gutman, D.; Krasnoperov, L. N. *J. Phys. Chem.* **1992**, *96*, 5881.
- (27) (a) Arican, H.; Arthur, N. L. *Aust. J. Chem.* **1983**, *36*, 2185. (b) Ferguson, K. C.; Pearson, J. T. *J. Chem. Soc., Faraday Trans.* **1970**, *66*, 910. (c) Trotman-Dickenson, A. F.; Steacie, E. W. R. *J. Chem. Phys.* **1950**,

18, 1097. (d) Dorfman, L. M.; Noyes, W. A., Jr. *J. Chem. Phys.* **1948**, *16*, 557. (e) Nicholson, A. J. C. *J. Am. Chem. Soc.* **1951**, *73*, 3981.

(26) Furue, H.; Pacey, P. D. *J. Phys. Chem.* **1990**, *94*, 1419. Marquaire, P.-M.; Dastidar, A. G.; Manthorne, K. C.; Pacey, P. D. *Can. J. Chem.* **1994**, *72*, 600. Bowdridge, M.; Furue, H.; Pacey, P. D. *J. Phys. Chem.*, in press.

(27) Johnston, H. S. *Gas Phase Reaction Rate Theory*; Ronald: New York, 1966.

(28) Lide, D. R., Ed. *Handbook of Chemistry and Physics*, 75th ed.; CRC Press: Boca Raton, FL, 1995; pp 5-26, 5-29, 9-69, 9-70.

(29) Thompson, H. B. *J. Chem. Phys.* **1967**, *47*, 3407.

(30) Pitzer, K. S. *J. Chem. Phys.* **1946**, *14*, 239.

(31) Swalen, J. D.; Costain, C. C. *J. Chem. Phys.* **1959**, *31*, 1562.

(32) Shimanouchi, T. *Tables of Molecular Vibrational Frequencies*; U.S. Department of Commerce: Washington, DC, 1972; Vol. 3, NSRDS-NBS39.

(33) (a) Herzberg, G. *Proc. R. Soc. London* **1961**, 262A, 291. (b) Snelson, A. J. *J. Phys. Chem.* **1970**, *74*, 537. (c) Milligan, D. E.; Jacox, M. E. *J. Chem. Phys.* **1967**, *47*, 5146. (d) Tan, L. Y.; Winer, A. M.; Pimentel, G. J. *J. Chem. Phys.* **1972**, *57*, 4028.

(34) Knyazev, V. D.; Benscira, A.; Stoliarov, S. I.; Slagle, I. R. Private communication, 1995.

JP9520613